An MD-study on changing the elemental distribution and composition by alloying to control front propagation in Al-Ni multilayers

Originally published in:
Journal of Applied Physics 132(6), https://doi.org/10.1063/5.0098254

Journal of Applied Physics ARTICLE scitation.org/journal/jap

An MD-study on changing the elemental distribution and composition by alloying to control front propagation in Al–Ni multilayers

Cite as: J. Appl. Phys. 132, 065101 (2022); doi: 10.1063/5.0098254
Submitted: 6 May 2022 · Accepted: 15 July 2022 ·
Published Online: 8 August 2022

Fabian Schwarz[a] and Ralph Spolenak

AFFILIATIONS

Laboratory for Nanometallurgy, Department of Materials, ETH Zürich, CH-8093 Zürich, Switzerland

[a]Author to whom correspondence should be addressed: fabian.schwarz@mat.ethz.ch

ABSTRACT

To cover the wide range of applications of reactive multilayers, it is necessary to have the ability to vary and control their front propagation velocities as well as their maximum reaction temperatures. In this paper, Molecular Dynamics simulations are used to study the influence of Al alloying, Ni alloying, and Co alloying on Al–Ni multilayers. In the case of alloying with Al and Ni, the iso-stoichiometric case where both the Al and the Ni layers are alloyed is first studied. In the second step, the stoichiometry is varied by alloying only one of the two layers with the other element. This allows for achieving very small front propagation velocities. Furthermore, the Ni layer is alloyed with Co and the whole range from a binary Al–Ni to the binary Al–Co system is studied. The front propagation velocity does not change linearly with the alloying fraction and reaches a minimum where the Ni/Co alloy changes from a face centered cubic to a hexagonal close packed lattice.

I. INTRODUCTION

Binary reactive multilayer nanofoils (RMNFs) have the property that they can locally release large amounts of energy in a short time. This energy is released when the individual layers, each consisting of a single metal, thermite, or Si,[1] start to inter-diffuse and eventually intermix. The process is started by locally heating the system and, thus, igniting the self-sustaining reaction. For this process to work, two materials with a big enthalpy of mixing are chosen. Examples include many aluminides, such as Al–Pt,[2] Al–Ni,[3] or Al–Ti,[4] but also many other binary systems, such as Ni–Ti[5] or Nb–Si.[6] Potential applications include thermal batteries,[7] reaction-assisted diffusion bonding,[8] the self-healing of metals,[9] MEMS waver level packaging,[10] and reactive wafer bonding.[11]

To tailor the reactive multilayer to a specific application, the ability to control the front propagation velocity, v_f, as well as the combustion temperature, T_c, is vital. As a consequence, the field of reactive multilayers is constantly investigating new ways to control the front propagation while also trying to better understand the underlying mechanisms of the reaction front propagation. A number of approaches are sketched in Fig. 1. In many systems, such as the Al–Ni system, the front propagation can be controlled by varying the bilayer height $h = h_{Al} + h_{Ni}$[12] [height of one Al layer plus the height of one Ni layer, see Fig. 1(a)] or the stoichiometry[3] [Fig. 1(b)], i.e., the ratio of the number of Al atoms to the number of Ni atoms. The front propagation can also be controlled by changing the system's architecture, for example, by depositing low-density compacts of multilayer reactive particles[13] or by depositing the multilayers onto a 3D printed architecture.[14] Finally, it is also possible to influence the front propagation velocity by varying the heat loss through the substrate[15] or by varying the substrate architecture,[16] as illustrated in Fig. 1(i).

Molecular Dynamics (MD) simulations have become a widely used tool to study reactive multilayers.[22] While they only allow to study comparably small systems, one has atomistic control over the system, its geometry and its properties. This means that not only the front propagation, but also the underlying diffusion and crystallization mechanisms can be studied. The vast majority of MD simulations of reactive multilayers focus on the Al–Ni model system.[23–25] Structurally, the influence of grain boundaries on the inter-diffusion at the Al–Ni interface,[26] the influence of the grain

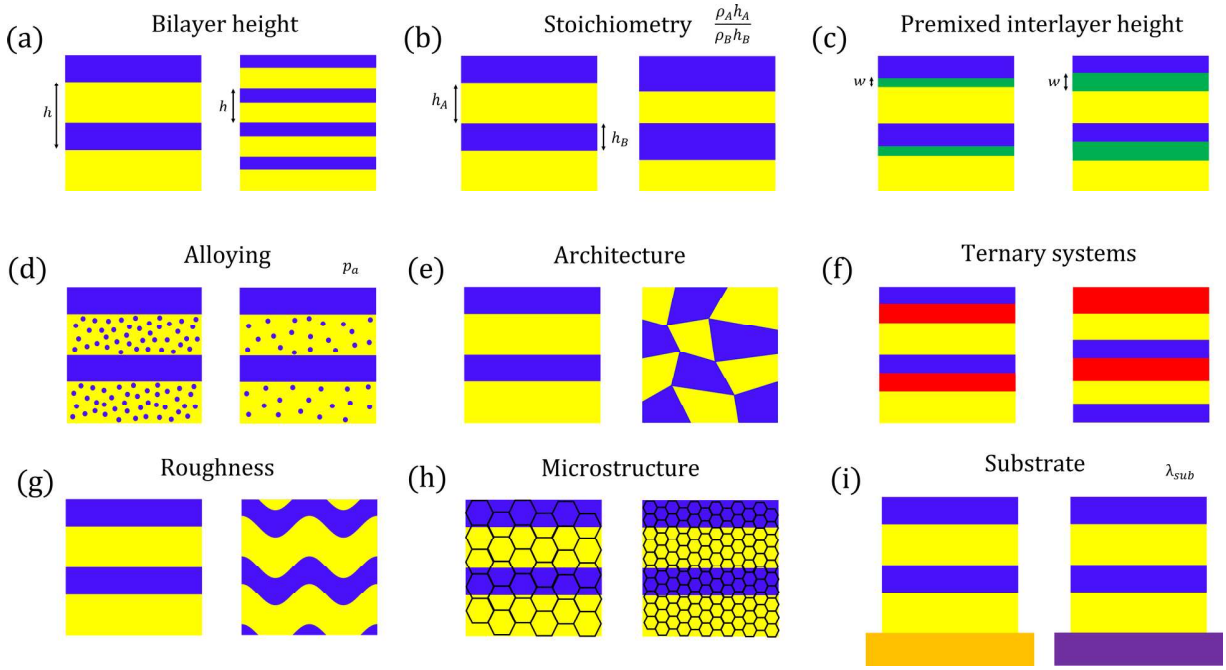

FIG. 1. Illustration of different approaches to control the front propagation velocity: (a) changing bilayer height,[12] (b) changing stoichiometry,[3] (c) changing premixed interlayer height,[17] (d) alloying,[18] (e) architecture,[13,14] (f) ternary systems,[19,20] (g) roughness, (h) microstructure,[21] and (i) changing the substrate.[15]

size on the front propagation,[27] and the influence of the microstructure on the front propagation velocity[21] have been studied recently [see Fig. 1(h)]. Geometrically, beyond multilayers, the front propagation in nanocrystals has been studied.[28] Furthermore, one can also study defects, such as the influence of the vacancy concentration on the front propagation reaction.[29] Moreover, most recently, the influence of premixed interlayers and how they can be used to control the reaction front propagation has been studied[17] [see Fig. 1(c)]. In this study, it was shown that in the Al–Ni system, the reaction is driven by a combination of the intermixing of the layers as well as the crystallization of the mixed AlNi to B2-AlNi.

In MD simulations, so far only binary systems have been studied. In the experiment, there have also been studies on ternary systems, such as Al–Ti–Si[20] or Al–Ru–Ni/Pt/Hf.[19] In this case, the multilayer consists of repeating units of three different pure layers, as illustrated in Fig. 1(f). Another way to introduce a third element is alloying. Danzi *et al.*[18] have studied alloying in the Al–Ni system by alloying the Ni layer with either Cu or Pt. This allows for architecture-independent reactivity tuning, which means access to a wide range of propagation velocities as well as combustion temperatures. To choose the different elements for the alloying systems, one would choose two different binary systems with different reactivities which have one common element (for example, Al in Al–Ni and Al–Pt) and then alloy the two elements that are different in the two systems.

In this work, the Al–Ni system which is the most widely studied system both experimentally and with MD simulations as well as the Al–Co system are chosen. The Al–Co system has also been studied experimentally,[30,31] but never in MD simulations. This study will investigate how alloying Ni with Co allows to tune the front propagation velocity. Furthermore, the concept of alloying with both Al and Ni is also studied. In that case, there are two main approaches. In the first one, both the Al and Ni layers are alloyed with the other element, varying the elemental distribution while keeping the stoichiometric ratio constant. In the second approach, either only the Al layer is alloyed with Ni or only the Ni layer is alloyed with Al. The latter approach changes the stoichiometry of the system and, thus, allows to control the front propagation velocity over a wider range.

II. SIMULATION DETAILS

The Large-scale Atomic/Molecular Massively Parallel Simulator (LAMMPS) package[32] was used to run the Molecular Dynamics (MD) simulations. To study alloying in the Al–Ni system, the interatomic forces were calculated using the Embedded Atom Method (EAM) force field by Pun and Mishin.[33] It has been the standard force field for MD simulations of Al–Ni RMNFs. The Al phase, the Ni phase, their inter-diffusion, as well as the intermetallic phases of Al and Ni are reproduced well. Furthermore, the potential's thermal and kinetic properties have been well investigated[34] and the resulting front propagation velocities have been compared to experiment.[17] Thus, it has been proven to be a good tool to study reactive Al–Ni multilayers. To study the Co alloying, the Ni–Al–Co EAM force field by Mishin and co-workers[35] was

used. This force field is based on the binary Al–Ni EAM force field by Mishin *et al.* and has been constructed such that the Al–Ni interactions are exactly the same as in the binary potential. The ternary potential has been constructed to reproduce the B2-NiAlCo phases well up to at least 1400 K. Thus, it reproduces well all the inter-metallic phases involved in the alloyed reactive multilayer systems. The properties of the force field together with the results of this paper are a first indication that it is well suited to study Al–Ni and Al–Co as well as Al–Ni_x/Co_{1-x} reactive multilayers.

The dimensions of the systems were kept constant at $L \times d \times h$. The length of the system, which is aligned in the x-direction, was chosen as $L = 430$ nm. The depth of the system, which is aligned in the y-direction, was chosen as $d = 1.4$ nm. Finally, the height of the system, which is aligned in the z-direction and equivalent to the bilayer-height was chosen as $h = 15$ nm. To study the Al–Co system in more detail, systems with a bilayer height in the range of [7.25, 10, 15, 25, 50 nm] were studied. Shrink-wrapped boundary conditions were imposed in the x-direction, which is equivalent to a free face at $x = 0$ nm and at $x = L$. Periodic boundary conditions were applied in y- and z-directions, which is equivalent to an infinitely deep and infinitely high multilayer. Such a system is comparable to the center of an experimental multilayer, which usually have a height of 50 or more bilayers and a width of several millimeters.

Every system is made up of columnar grains with a constant grain size equal to the height of a Ni layer $h_{Ni} = h - h_{Al} \approx 6$ nm, which is comparable to grain structures that have been observed experimentally.[36,37] For Al–Co systems, the grain size was chosen in the same way and set to the height of one Co layer $h_{Co} = h - h_{Al}$. The columnar grain structure was created using a Voronoi tessellation within the framework of the Open Source command-line program Atomsk.[38] The crystallographic orientation of the grains varies from grain to grain in the x-direction and was chosen randomly, while the orientation is the same for all the grains that are aligned in the z-direction (any two grains, whose range along the x-direction is the same, have the same orientation). The initial stoichiometric ratio between Al and Ni atoms was chosen as 1. Finally, an amorphous premixed interlayer of height $w = 2$ nm was introduced at the interface between Al and Ni, which is in agreement with previous experimental[12] as well as MD[17] studies.

To create the Al- and Ni-alloyed systems, Al atoms in the Al layer were simply replaced by Ni atoms and vice versa. The alloying fraction was varied from 0 to 50%. The system with an alloying fraction of 50% corresponds to a fully mixed AlNi system. In the non-stoichiometric case, only either Al atoms or Ni atoms were replaced. Here, the alloying fraction was varied between 30 and 60 at. % Al. This range was chosen, as outside of this range, there is no self-propagating reaction. For the Co alloying, Ni atoms in the Ni layer, as well as in the premixed interlayer, were replaced by Co atoms. In this case, the full range between 0 and 100 at. % Co in the Ni/Co layer was studied. The different systems are illustrated in Fig. 2.

After creation, the systems were equilibrated in an NPT ensemble (constant number of particles, constant pressure, constant temperature) at $T_0 = 300$ K for 0.4 ns. The self-propagating reaction was then ignited by heating up the system at $x < 50$ nm to 1400 K in an NPT ensemble (constant number of particles, constant pressure, constant temperature). At the same time, the system at $x > 100$ nm was kept at $T_0 = 300$ K in an NPT ensemble, while the system at 50 nm $< x <$ 100 nm evolved in an NP$\mathcal{H}$ ensemble (constant number of particles, constant pressure, constant enthalpy). The average pressure of the barostat was always set to 0 Pa. This setup allows for creating a realistic temperature distribution after ignition. The self-propagating reaction was then studied by letting the system evolve in an NP$\mathcal{H}$ ensemble for 6 ns.

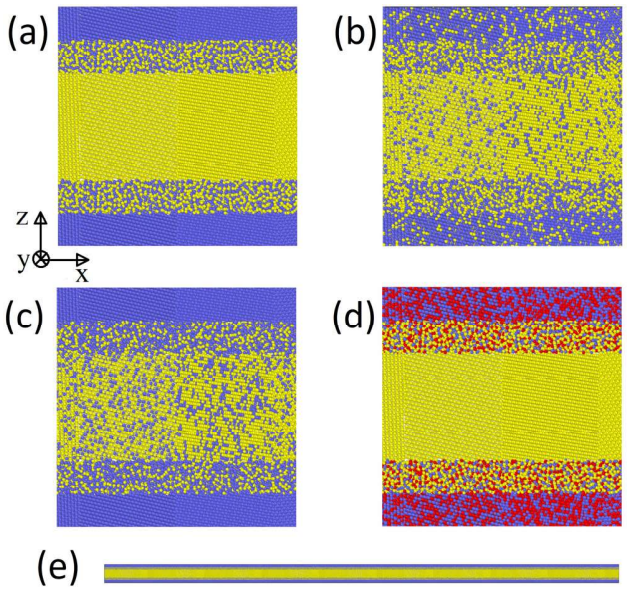

FIG. 2. (a)–(d) Magnification of different systems: (a) initial system, (b) changing the elemental distribution by Al and Ni alloying, (c) non-stoichiometric Ni alloying, and (d) Co alloying. Al atoms are in yellow, Ni atoms in blue, and Co atoms in red. (e) The full size initial system.

To measure the front propagation velocity v_f, the position of the reaction front was recorded every 0.2 ns. The position of the front was defined as the point where the temperature is equal to 1042 K, which is the melting temperature of Al in the EAM force field (see Fig. 3). The temperature profile is obtained by 1D binning of the temperature using 100 bins. At the center of every bin, the temperature is defined as the average temperature of the bin while in between, a linear interpolation is used. In accordance with previous publications,[17,21] the time step was chosen as 2 fs. The damping parameter for the pressure was chosen as 2 ps, while the damping parameter for the temperature was chosen as 0.2 ps. To visualize the system with respect to atom type or crystal structure, the open Open Source scientific visualization and analysis software OVITO[39] was used.

III. RESULTS

The alloying fraction is varied for the two types of Al and Ni alloying as well as for the Co alloying (see Fig. 2). Then, the change

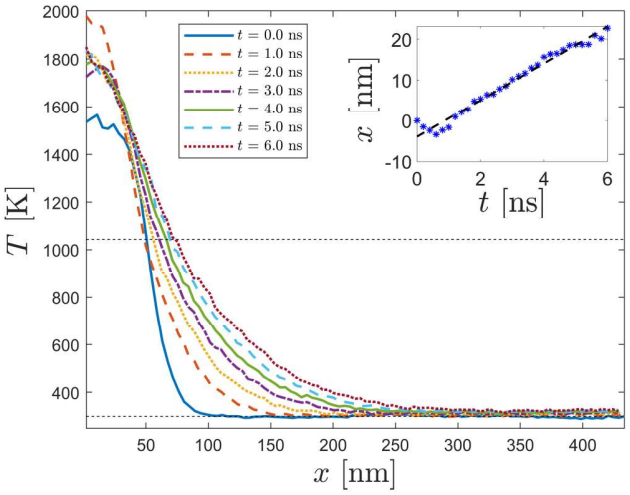

FIG. 3. Temperature distribution at different times of the Al–Co system. The horizontal dashed line represents the melting temperature of Al, where the position of the reaction front is defined. Inset: Normalized front position vs time, the slope of a linear fit determines the propagation velocity v_f.

of the front propagation velocity v_f with the alloying fraction is reported and diffusion mechanisms are described and illustrated.

A. Aluminum and nickel alloying

In the first set of simulations, both the Al layer and the Ni layer are alloyed with the respective other element. The alloying fraction p_a is varied from 0 (initial system) to 0.5 (fully intermixed system) in steps of 0.1. The relationship between the alloying fraction and the front propagation velocity is illustrated in Fig. 4(a). First, the front propagation velocity decreases with increasing alloying fraction, before reaching a minimum at $p_a = 0.3$ and then increases again.

The diffusion mechanism in the system without alloying can be divided into five stages as follows: (i) Some individual atoms start diffusing from the premixed interlayer into the Al grain boundaries. (ii) The Al layer is melting at the reaction front. At the same time, the premixed interlayer partially crystallizes into B2-AlNi. (iii) Just behind the reaction front, atoms from the premixed interlayer diffuse into the molten Al through volume diffusion and into Ni grain boundaries. (iv) A bit further behind the reaction front, the Ni layer starts to diffuse into the crystallized (polycrystalline) premixed interlayer. (v) At the back of the reaction front, all AlNi crystallizes to B2-AlNi.

With increasing alloying fraction, it can be observed that the crystallized premixed interlayer starts growing. At higher alloying fractions, the Al and Ni layers do not fully intermix anymore. Finally, at $p_a = 0.5$, the system is a fully intermixed AlNi system. As the fcc AlNi phase is very unstable, the full system immediately undergoes amorphization. This means that the reaction is completely driven by the crystallization from amorphous AlNi to B2-AlNi. The system with $p_a = 0.3$ is shown in Figs. 5(a) and 5(b).

In the second set of simulations, only either the Al layer is alloyed with Ni (Al at.% $< 50\%$) or the Ni layer is alloyed with Al (Al at.% $> 50\%$). The atom percentage of Al is varied from 30% to 60% in steps of 5%, as outside of this range there is no self-sustaining reaction. The change in front propagation velocity with changing Al atom percentage is illustrated in Fig. 4(b). The front velocity has a maximum at an Al atom percentage of 45%. For higher Al atom percentages, the front velocity quickly decreases down to zero at an Al atom percentage of 60%. In the Ni-rich zone, the decrease in front propagation velocity has a similar slope and shape and goes down to zero at an Al atom percentage of 30%.

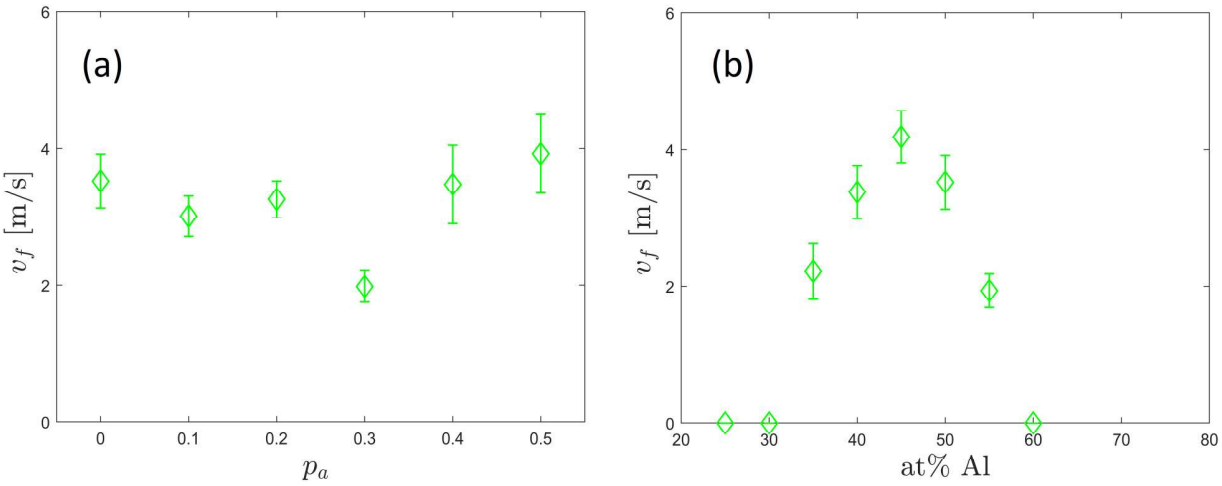

FIG. 4. (a) Plot of the front propagation velocity v_f vs the alloying fraction p_a in the iso-stoichiometric Al and Ni alloying. (b) Plot of the front propagation velocity v_f vs the Al atomic percentage in the non-stoichiometric alloying with Al or Ni, respectively. The error bars represent the fitting error of the linear fit of the front position vs time.

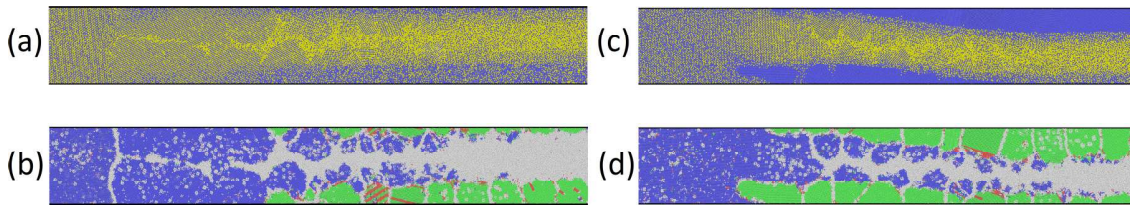

FIG. 5. [(a) and (b)] Al- and Ni-alloying system of the first kind with $p_a = 0.3$. [(c) and (d)] Ni-alloying system of the second kind with Al at. % = 35%. [(a) and (c)] Coloring by atom type (Al: yellow, Ni: blue) and [(b) and (d)] coloring by crystal structure (fcc: green, bcc: blue, hcp: red).

With regard to the diffusion processes, the crystallized premixed interlayer is also growing as the Al atom percentage deviates from 50%. Moreover, the non-alloyed layer does not completely diffuse into the other layer. Finally, for large deviations from an Al atom percentage of 50%, also the alloyed layer does not fully intermix anymore. Figures 5(c) and 5(d) show the system with an Al atom percentage of 35%.

B. Cobalt alloying

Before studying Co alloying, the change in front propagation velocity with varying bilayer height in binary Al–Co systems is studied. The height of the premixed interlayer was chosen as $w = 2$ nm, just as in the Al–Ni system. Results are shown in Fig. 6. The MD simulations are compared with experiments by Adams *et al.*[30] While, due to the lack of electron heat transport in MD simulations and just as in the Al–Ni system,[17] the peak is shifted to lower bilayer heights and the reaction is quenched already below bilayer heights of 50 nm, MD simulations manage to reproduce the characteristic shape of the front velocity vs bilayer height curve. This is a further indication that the Ni–Al–Co force field can be used to study alloying of the Al–Ni system with Co.

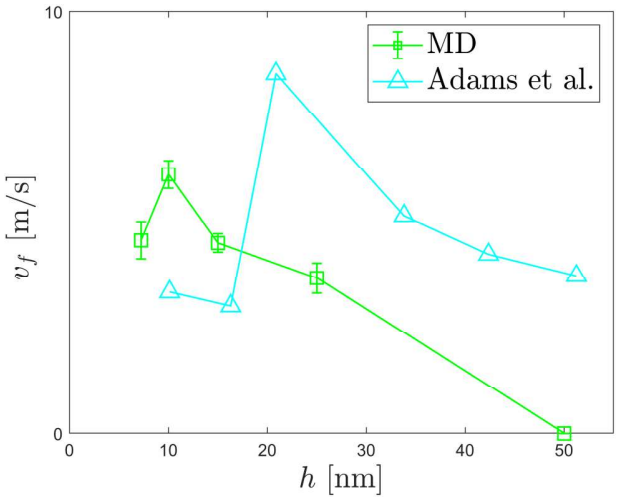

FIG. 6. Plot of bilayer height h vs front propagation velocity v_f for Al–Co multilayers with a premixed interlayer height of $w = 2$ nm. For comparison, MD results are compared to experimental data from Adams *et al.*[30]

In the third set of alloying simulations, the Ni layer is alloyed with Co. The atom percentage of Co in the Ni layer is varied from 0% to 100% in steps of 10%. An additional system at a Co atom percentage of 65% is studied, as this is very close to the point in the phase diagram where NiCo changes from cubic to a hexagonal crystal structure (≈67 at.% Co). Figure 7(a) shows the change in the front propagation velocity with changing Co atom percentage in the Ni layer. At first, the propagation velocity slightly increases until a Co atom percentage of 30%, then it decreases and reaches a minimum at the point where the crystal structure of the NiCo layer changes from fcc to hcp. When further increasing the Co content, the front propagation velocity steadily increases and reaches a maximum at the binary Al–Co system. The change in enthalpy with changing Co atom percentage is plotted in Fig. 7(b). The enthalpy of both the unreacted and the fully intermixed system first decreases with increasing Co content, before reaching a minimum between 50% and 60% Co in the NiCo layer. When further increasing the Co content, the enthalpy increases again and reaches a maximum at 100% cobalt. The enthalpy of crystallization is minimal in the region between 65% and 80% Co.

The diffusion processes in the Al–Co system are very similar to those in the Al–Ni system. There are, however, two small differences. First, in the Al–Co system, the atoms from the premixed interlayer start diffusing into the Co grain boundaries already at the reaction front and not just behind it, as in the Al–Ni system. Second, the cubic AlCo phase that forms behind the reaction front is of a layered fashion, as illustrated in Fig. 8(d).

When varying the Co atom percentage, the premixed interlayer is only partially crystallizing. Moreover, behind the reaction front, only B2-AlNi is forming with Co atoms aggregating in-between the B2-AlNi grains, as illustrated with the system with Co at.% = 50% in Figs. 8(a) and 8(b).

IV. DISCUSSION

When equally alloying the Al and Ni layer with the respective other element (and, thus, keeping the stoichiometric ratio constant), the front propagation velocity first decreases up to an alloying fraction of $p_a = 0.3$, before increasing again up to the maximum alloying fraction. This behavior can be explained when considering the two main energy sources that fuel the front propagation:

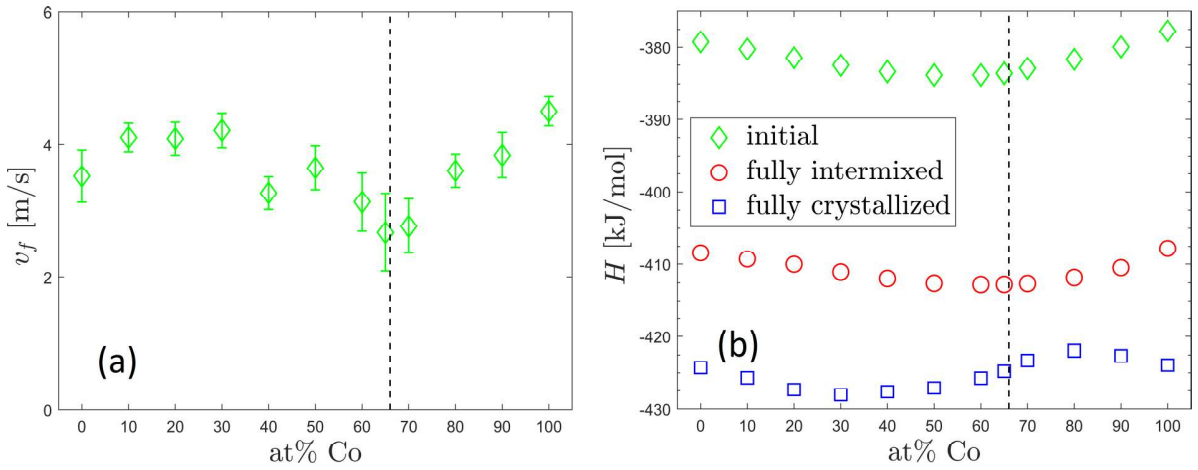

FIG. 7. (a) Plot of the front propagation velocity v_f vs the atomic percentage of Co in the Ni/Co layer. The error bars represent the fitting error of the linear fit of the front position vs time. (b) Plot of the enthalpy of the initial system at 300 K, the fully intermixed system at 300 K as well as the fully crystallized system at 300 K vs the atomic percentage of Co in the Ni/Co layer. In both plots, the horizontal dashed line represents the point in the phase diagram where the crystal structure of NiCo changes from fcc to hcp.

(i) The heat of mixing created by the intermixing of Al and Ni. (ii) The heat of crystallization created by the intermixed AlNi crystallizing to B2-AlNi. The heat of mixing decreases with increasing alloying fraction, which is why the front propagation velocity is initially decreasing. On the other hand, for high alloying fractions, there is hardly any intermixing and the front propagation is mainly driven by crystallization of B2-AlNi. So while the intermixing provides energy to the front propagation reaction, it can also slow down the reaction as the crystallization reaction can only happen once the intermixing has taken place.

By only alloying one of the two layers, either the Al layer with Ni or the Ni layer with Al, the stoichiometric ratio is changed. The maximum of propagation velocity is observed at an Al atomic percentage of 45%, and it drops almost symmetrically down to zero at an Al atomic percentage of 30% and 60%, respectively. The circumstance that the maximum is off-center is likely due to the fact that the front propagation velocity is influenced by the combination of the intermixing time as well as the energy generated through intermixing. As the intermixing time is mainly governed by the thickness and melting point of the lower melting point layer, in this case the Al layer, the intermixing time is likely inversely proportional to the thickness of the Al layer. This might be the reason that at 45 at. % Al, the front propagation velocity is higher than at 50 at. % Al, even though the heat of mixing decreases. The drop in front propagation velocity on either side of the maximum can then mainly be attributed to the decrease in heat of mixing and heat of crystallization. Both should decrease linearly with $|p_{Al} - 0.5|$, where p_{Al} is the atomic fraction of Al atoms.

For the binary Al–Ni system, the most promising experimental road to control the front propagation velocity over a wide range would be to either alloy the Ni layer with Al or the Al layer with Ni. This should be achievable in vapor deposition by simply co-sputtering Al and Ni to create layers with the desired alloying fraction. Due to the lower melting point of the pure Al layer, it is very likely that on the Al-rich side, one would access lower ignition temperatures, while on the Ni-rich side, the ignition temperatures should be slightly higher. A further route would be to alloy both layers, but with different alloying fractions, which might allow for

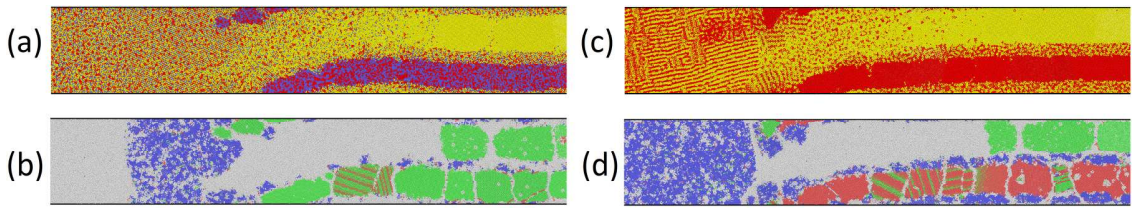

FIG. 8. [(a) and (b)] Al–Ni/Co system with Co at.% = 50%. [(c) and (d)] Al–Co system. [(a) and (c)] coloring by atom type (Al: yellow, Ni: blue, Co: red) and [(b) and (d)] Coloring by crystal structure (fcc: green, bcc: blue, hcp: red).

faster deposition times, as both targets could be left open at all times and only the power would have to be changed.

In the system where the Ni layer is alloyed with Co, the front propagation velocity first slightly increases with the Co concentration, before it goes down to a minimum, which is located at the transition of NiCo from fcc to hcp, i.e., the concentration of zero stacking fault energy. After the minimum, it steadily increases up to the maximum front propagation velocity, which was found for the Al–Co system. The change in enthalpy of mixing across the whole range of NiCo intermetallics is below 2 kJ/mol [see Fig. 7(b)]. For the Molecular Dynamics Al–Ni system, the heat of crystallization was measured to be 16 kJ/mol. In the binary systems, the whole system can crystallize to a bcc phase behind the reaction front, while for intermetallics, only part of the system crystallizes to a bcc AlNi or a bcc AlCo, respectively. As a result, the observed maximum difference in heat of crystallization is on the order of 7 kJ/mol [17.3 kJ/mol for 20% Co, 10.1 for 80% Co, see Fig. 7(b)]. While this suggests that the difference in propagation velocity can be explained largely by the change in enthalpy of crystallization, there also seems to be an influence on the rate of diffusion. The slight increase in propagation velocity for small Co alloying fractions could be explained by a slightly higher heat of crystallization, the reduced crystallization of the premixed interlayer, and with the fact that Co seems to aid diffusion. This could also be the reason for the fact that the front propagation velocity in the Al–Co system is higher than in the Al–Ni system. Recent studies have also shown that the microstructure can influence the front propagation velocity.[21] As Co has an hcp crystal structure and Ni has an fcc crystal structure, this could be another contributing factor to the difference in front propagation velocity.

If one tries to imagine a system, where the range over which the front propagation velocity can be tuned is maximized, one would start with a binary system that has a very high front propagation velocity, such as Al–Pt.[2] One would then alloy one layer with the other element, in the case of Al–Pt, one could alloy the Al layer with Pt. This should give access to a range of the front propagation velocity from 0 up to the maximum front propagation velocity, which is around 90 ms^{-1}.[40] Another approach would be to alloy one layer with an element that has a melting temperature far beyond the combustion temperature of the reactive multilayer. This approach has already been shown to work in the Al–Ni system, where Schnabel *et al.* alloyed the Ni layer with Nb.[41]

With respect to diffusion, it was found that when equally alloying both layers with Al and Ni, respectively, an increase in the alloying fraction will lead to growth of the crystallized interlayer. As this crystallized interlayer acts as a diffusion barrier, the interdiffusion through the crystallized interlayer is slowed down, the higher the alloying fraction. Already at an alloying fraction of $p_a = 0.3$, not all atoms are diffusing through the crystallized interlayer and, thus, there is no complete intermixing anymore. A similar, but weaker effect of the growth of the premixed interlayer on the diffusion can also be observed when only one of the layers is alloyed. The effect is weaker, as the crystallized interlayer only grows on the side of the alloyed layer. However, in that case, the excess of atoms of the type of the non-alloyed layer increases the effect of the incomplete intermixing, which eventually leads to the absence of a self-propagating reaction for large deviations from 45% Al.

In the Al–Co system, atoms from the premixed interlayer are diffusing more easily into Co grain boundaries than atoms are diffusing into the Ni grain boundaries in the Al–Ni system. This might well be due to the fact that the grain boundary energy of Co is significantly higher than that of Ni.[42] This also leads to a higher diffusion coefficient for Co in comparison to Ni.[43] Furthermore, alloying the Ni layer with Co inhibits the crystallization of the interlayer, which aids diffusion through the interlayer.

V. CONCLUSIONS

The influence of both Al and Ni alloying and Co alloying in the Al–Ni reactive multilayer has been investigated. It was shown that equally alloying the Al and the Ni layer with the respective other element only gives small control over the front propagation velocity. The reason for this is that increasing the alloying fraction in this system means decreasing the enthalpy of mixing, but at the same time the crystallization from amorphous AlNi to B2-AlNi is aided by the increasing alloying fraction, as a larger proportion of the system can crystallize without requiring previous interdiffusion and intermixing.

Alloying only one layer with the respective other element (which means changing the overall stoichiometry) is shown to give control over a wide range of propagation velocities from 0 to above 4 ms^{-1}. The maximum propagation velocity is observed at an atomic percentage of 45% Al. The propagation velocity can then be tuned by varying the Al percentage either between 30% and 45% or between 45% and 60%. The main reason for the sharp decrease in propagation velocity is the reduced heat of mixing. If one aims to further increase the range of propagation velocities, one could change the bilayer height to maximize the velocity. In the Al–Ni system, the maximum of propagation velocity was experimentally found to be at a bilayer height of around $h = 20$ nm.[12] The range can be further increased by choosing a different system with higher reactivity and, thus, higher maximum propagation velocity, such as Al–Pt.

When alloying with a third element, Co in the case of this study, it was shown that the front propagation velocity does not necessarily have to increase steadily. This work has found a minimum of propagation velocity when the Ni layer is alloyed with about 66% of Co. Putting this into perspective, the effect of alloying is highly dependent on the reactivity of the alloying element with the non-alloyed layer. Choosing a highly reactive element such as Pt will allow to increase the front propagation velocity, while choosing a weakly reactive element such as Nb will allow to decrease the front propagation velocity. However, this work suggests that alloying one of the two layers with the respective other element in a binary system is the best way to access a wide range of front propagation velocities. There are, however, still many reasons to include a third chemical element for alloying. First, producing systems with layers that are only alloyed with the respective other element from the bilayer might be a hard task experimentally. Second, the alloying element might be much cheaper and will thus decrease the overall cost of the system. Third, the area of application might also favor the addition of a third element, for example,

for stability reasons. Finally, by adding the right additional element, one can increase the window, in which the alloying does still lead to a system that does not quench, allowing for larger error tolerances when producing the multilayers.

In conclusion, alloying in reactive multilayers using MD simulations was studied. Furthermore, it was confirmed that alloying can be used for architecture-independent tuning of the propagation velocity. With respect to the underlying mechanisms, MD simulations show that both changes in the diffusion process and changes in the heat of mixing and the heat of crystallization play a role. Finally, when the goal is to maximize the range in which the front propagation velocity can be varied, it was shown that whenever possible, one should stay with a binary system and try to alloy only one layer with the respective other element, rather than introducing a further element. Furthermore, it can also serve as a guideline for experimental studies with regard to the relevant stoichiometry window.

AUTHOR DECLARATIONS

Conflict of Interest

The authors have no conflict to disclose.

Author Contributions

Fabian Schwarz: Conceptualization (equal); Investigation (lead); Methodology (lead); Visualization (lead); Writing – original draft (lead); Writing – review and editing (lead). **Ralph Spolenak:** Conceptualization (equal); Supervision (lead); Writing – review and editing (supporting).

DATA AVAILABILITY

The data that support the findings of this study are available from the corresponding author upon reasonable request.

REFERENCES

[1]D. Adams, "Reactive multilayers fabricated by vapor deposition: A critical review," Thin Solid Films **576**, 98–128 (2015).
[2]D. P. Adams, R. V. Reeves, M. J. Abere, C. Sobczak, C. D. Yarrington, M. A. Rodriguez, and P. G. Kotula, "Ignition and self-propagating reactions in Al/Pt multilayers of varied design," J. Appl. Phys. **124**, 095105 (2018).
[3]T. S. Dyer and Z. A. Munir, "The synthesis of nickel aluminides by multilayer self-propagating combustion," Metall. Mater. Trans. B **26**, 603–610 (1995).
[4]J.-C. Gachon, A. Rogachev, H. Grigoryan, E. Illarionova, J.-J. Kuntz, D. Kovalev, A. Nosyrev, N. Sachkova, and P. Tsygankov, "On the mechanism of heterogeneous reaction and phase formation in Ti/Al multilayer nanofilms," Acta Mater. **53**, 1225–1231 (2005).
[5]D. P. Adams, M. A. Rodriguez, J. P. McDonald, M. M. Bai, E. Jones, L. Brewer, and J. J. Moore, "Reactive Ni/Ti nanolaminates," J. Appl. Phys. **106**, 093505 (2009).
[6]M. Reiss, C. Esber, D. Van Heerden, A. Gavens, M. Williams, and T. Weihs, "Self-propagating formation reactions in Nb/Si multilayers," Mater. Sci. Eng., A **261**, 217–222 (1999).
[7]Y. Zhu, J. Geng, F. Wang, S. Yan, P. Zhao, Q. Meng, J. Wang, and Q. Wu, "Preparation of Al/Ni reactive multilayer foils and its application in thermal battery," Z. Anorg. Allg. Chem. **646**, 200–206 (2020).
[8]A. Cavaleiro, A. Ramos, F. Braz Fernandes, N. Schell, and M. Vieira, "Follow-up structural evolution of Ni/Ti reactive nano and microlayers during diffusion bonding of niti to Ti6Al4V in a synchrotron beamline," J. Mater. Process. Technol. **275**, 116354 (2020).
[9]S. Danzi, V. Schnabel, J. Gabl, A. Sologubenko, H. Galinski, and R. Spolenak, "Self-healing electronics: Rapid on-chip healing of metal thin films," Adv. Mater. Technol. **4**, 1970015 (2019).
[10]X. Qiu, J. Zhu, J. Oiler, and H. Yu, "Reactive multilayer foils for MEMS wafer level packaging," in *2009 59th Electronic Components and Technology Conference* (IEEE, 2009), pp. 1311–1316.
[11]K. Vogel, S. Braun, C. Hofmann, M. Weiser, M. Wiemer, T. Otto, and H. Kuhn, "Reactive bonding," in *3D and Circuit Integration of MEMS* (John Wiley & Sons, Ltd., 2021), Chap. 14, pp. 309–329.
[12]R. Knepper, M. R. Snyder, G. Fritz, K. Fisher, O. M. Knio, and T. P. Weihs, "Effect of varying bilayer spacing distribution on reaction heat and velocity in reactive Al/Ni multilayers," J. Appl. Phys. **105**, 083504 (2009).
[13]G. M. Fritz, H. Joress, and T. P. Weihs, "Enabling and controlling slow reaction velocities in low-density compacts of multilayer reactive particles," Combust. Flame **158**, 1084–1088 (2011).
[14]K. T. Sullivan, C. Zhu, E. B. Duoss, A. E. Gash, D. B. Kolesky, J. D. Kuntz, J. A. Lewis, and C. M. Spadaccini, "Controlling material reactivity using architecture," Adv. Mater. **28**, 1934–1939 (2016).
[15]S. Danzi, M. Menétrey, J. Wohlwend, and R. Spolenak, "Thermal management in Ni/Al reactive multilayers: Understanding and preventing reaction quenching on thin film heat sinks," ACS Appl. Mater. Interfaces **11**, 42479–42485 (2019).
[16]B. Julien, P. Dubreuil, C. Josse, L. Salvagnac, S. Pelloquin, A. Esteve, and C. Rossi, "Effect of substrate–induced localized stress on the combustion properties of Al/CuO reactive multilayer films," Thin Solid Films **740**, 139000 (2021).
[17]F. Schwarz and R. Spolenak, "The influence of premixed interlayers on the reaction propagation in Al–Ni multilayers—An MD approach," J. Appl. Phys. **131**, 075107 (2022).
[18]S. Danzi, V. Schnabel, X. Zhao, J. Käch, and R. Spolenak, "Architecture-independent reactivity tuning of Ni/Al multilayers by solid solution alloying," Appl. Phys. Lett. **114**, 183102 (2019).
[19]C. Pauly, K. Woll, I. Gallino, M. Stüber, H. Leiste, R. Busch, and F. Mücklich, "Ignition in ternary Ru/Al-based reactive multilayers–effects of chemistry and stacking sequence," J. Appl. Phys. **124**, 195301 (2018).
[20]S. Sen, M. Lake, R. Grieseler, and P. Schaaf, "Effects of multilayer arrangement in ternary reactive film on self-propagating reaction properties," Surf. Coat. Technol. **327**, 25–31 (2017).
[21]F. Schwarz and R. Spolenak, "Molecular dynamics study of the influence of microstructure on reaction front propagation in Al–Ni multilayers," Appl. Phys. Lett. **119**, 133901 (2021).
[22]F. Baras, V. Turlo, O. Politano, S. G. Vadchenko, A. S. Rogachev, and A. S. Mukasyan, "SHS in Ni/Al nanofoils: A review of experiments and molecular dynamics simulations," Adv. Eng. Mater. **20**, 1800091 (2018).
[23]O. Politano and F. Baras, "Molecular dynamics simulations of self-propagating reactions in Ni–Al multilayer nanofoils," J. Alloys Compd. **652**, 25–29 (2015).
[24]V. Turlo, O. Politano, and F. Baras, "Modeling self-sustaining waves of exothermic dissolution in nanometric Ni-Al multilayers," Acta Mater. **120**, 189–204 (2016).
[25]A. Rogachev, S. Vadchenko, F. Baras, O. Politano, S. Rouvimov, N. Sachkova, M. Grapes, T. Weihs, and A. Mukasyan, "Combustion in reactive multilayer Ni/Al nanofoils: Experiments and molecular dynamic simulation," Combust. Flame **166**, 158–169 (2016).
[26]B. Witbeck and D. E. Spearot, "Role of grain boundary structure on diffusion and dissolution during Ni/Al nanolaminate combustion," J. Appl. Phys. **127**, 125111 (2020).
[27]B. Witbeck and D. E. Spearot, "Grain size effects on Ni/Al nanolaminate combustion," J. Mater. Res. **34**, 2229–2238 (2019).

[28]O. Politano and F. Baras, "Reaction front propagation in nanocrystalline Ni/Al composites: A molecular dynamics study," J. Appl. Phys. **128**, 215301 (2020).
[29]B. Witbeck, J. Sink, and D. E. Spearot, "Influence of vacancy defect concentration on the combustion of reactive Ni/Al nanolaminates," J. Appl. Phys. **124**, 045105 (2018).
[30]D. P. Adams, V. C. Hodges, M. M. Bai, E. Jones, M. A. Rodriguez, T. Buchheit, and J. J. Moore, "Exothermic reactions in Co/Al nanolaminates," J. Appl. Phys. **104**, 043502 (2008).
[31]R. V. Reeves and D. P. Adams, "Reaction instabilities in Co/Al nanolaminates due to chemical kinetics variation over micron-scales," J. Appl. Phys. **115**, 044911 (2014).
[32]S. Plimpton, "Fast parallel algorithms for short-range molecular dynamics," J. Comput. Phys. **117**, 1–19 (1995).
[33]G. P. Pun and Y. Mishin, "Development of an interatomic potential for the Ni-Al system," Philos. Mag. **89**, 3245–3267 (2009).
[34]V. Turlo, F. Baras, and O. Politano, "Comparative study of embedded-atom methods applied to the reactivity in the Ni–Al system," Modell. Simul. Mater. Sci. Eng. **25**, 064002 (2017).
[35]G. P. P. Pun, V. Yamakov, and Y. Mishin, "Interatomic potential for the ternary Ni–Al–Co system and application to atomistic modeling of the B2–$L1_0$ martensitic transformation," Modell. Simul. Mater. Sci. Eng. **23**, 065006 (2015).
[36]A. F. Jankowski, "Vapor deposition and characterization of nanocrystalline nanolaminates," Surf. Coat. Technol. **203**, 484–489 (2008), *Proceedings of the 35th International Conference on Metallurgical Coatings and Thin Films*.
[37]S. C. Kelly and N. N. Thadhani, "Shock compression response of highly reactive Ni+Al multilayered thin foils," J. Appl. Phys. **119**, 095903 (2016).
[38]P. Hirel, "Atomsk: A tool for manipulating and converting atomic data files," Comput. Phys. Commun. **197**, 212–219 (2015).
[39]A. Stukowski, "Visualization and analysis of atomistic simulation data with OVITO—The open visualization tool," Modell. Simul. Mater. Sci. Eng. **18**, 015012 (2010).
[40]D. Adams, M. Rodriguez, C. Tigges, and P. Kotula, "Self-propagating, high-temperature combustion synthesis of rhombohedral alpt thin films," J. Mater. Res. **21**, 3168–3179 (2006).
[41]V. Schnabel, A. S. Sologubenko, S. Danzi, G. Kurtuldu, and R. Spolenak, "Controlling diffusion in Ni/Al reactive multilayers by Nb-alloying," Appl. Phys. Lett. **111**, 173902 (2017).
[42]H. Zheng, X.-G. Li, R. Tran, C. Chen, M. Horton, D. Winston, K. A. Persson, and S. P. Ong, "Grain boundary properties of elemental metals," Acta Mater. **186**, 40–49 (2020).
[43]J. Pelleg, "On the relation between diffusion coefficients and grain boundary energy," Philos. Mag. A **14**, 595–601 (1966).